Journal of Power Sources 188 (2009) 588–591

Contents lists available at ScienceDirect

Journal of Power Sources

journal homepage: www.elsevier.com/locate/jpowsour

Short communication

Morphology effect on the electrochemical performance of NiO films as anodes for lithium ion batteries

X.H. Huang, J.P. Tu*, X.H. Xia, X.L. Wang, J.Y. Xiang, L. Zhang, Y. Zhou

Department of Materials Science and Engineering, Zhejiang University, Hangzhou 310027, China

ARTICLE INFO

Article history:
Received 24 October 2008
Received in revised form
27 November 2008
Accepted 28 November 2008
Available online 3 December 2008

Keywords:
NiO film
Morphology
Anode
Lithium ion battery

ABSTRACT

NiO films were prepared by chemical bath deposition and electrodeposition method, respectively, using nickel foam as the substrate. The films were characterized by scanning electron microscopy (SEM) and the images showed that their morphologies were distinct. The NiO film prepared by chemical bath deposition was highly porous, while the film prepared by electrodeposition was dense, and both of their thickness was about 1 μm. As anode materials for lithium ion batteries, the porous NiO film prepared by chemical bath deposition exhibited higher coulombic efficiency and weaker polarization and its specific capacity after 50 cycles was 490 mAh g^{-1} at the discharge–charge current density of 0.5 A g^{-1}, and 350 mAh g^{-1} at 1.5 A g^{-1}, higher than the electrodeposited film (230 mAh g^{-1} at 0.5 A g^{-1}, and 170 mAh g^{-1} at 1.5 A g^{-1}). The better electrochemical performances of the film prepared by chemical bath deposition are attributed to its highly porous morphology, which shorted diffusion length of lithium ions, and relaxed the volume change caused by the reaction between NiO and Li^+.

1. Introduction

Recently, lithium ion film batteries are widely used as the power supplies for the microcircuit of electronic products. Among these microbatteries, one kind of the promising anode material is the transition-metal oxides (MO, where M is Fe, Co, Ni, and Cu), which have been widely studied since they were first proposed by Tarascon and co-workers [1–6]. These films can be prepared by a variety of methods, such as the electrostatic spray deposition technique [7,8], pulsed laser ablation [9,10], chemical bath deposition [11–17], and electrodeposition [18–21]. These oxide films demonstrate high reversible capacities as high as 700 mAh g^{-1} and exhibit good cycling performances. However, many films are less than 500 nm in thickness, which contain too small quantity of active materials. If the film is thicker, the electrical conduction in the film is poorer and the diffusion length of lithium ions is longer as compared to the thinner film, which may lead to worse electrochemical properties. In this case, the morphology of the thick films should be taken into careful consideration, because it is closely related to the electrochemical performances. For example, for the porous thick film, the electrical conduction may be better and the diffusion length of lithium ions may be shorter as compared to the dense thick film. However, to our knowledge, not many investigations have been done on the morphology effect on the electrochemical performances of film electrode. So in the present work, two NiO films with distinct morphology were prepared, that are, a porous NiO film prepared by chemical bath deposition, and a dense NiO film prepared by electrodeposition, and their electrochemical properties were investigated.

2. Experimental

The NiO film by chemical bath deposition was prepared as follows. Solution for chemical bath deposition was obtained by mixing 40 mL of 1 M nickel sulfate, 30 mL of 0.25 M potassium persulfate, 10 mL of aqueous ammonia (25–28%), and 20 mL of deionized water in a beaker under stirring at room temperature. The nickel foam substrate with a size of 3 × 4 cm^2 was placed vertically in the solution and deposited for 1 h. After being washed and dried, the substrate was heat treated in a quartz tube furnace at 350 °C for 2 h in flowing argon.

The electrodeposited NiO film was prepared as follows. The electrolyte was composed of 1 M nickel nitrate and its pH value was adjusted to 1.5 with concentrated nitric acid. Nickel foam with a size of 3 × 4 cm^2 was used as the working cathode and nickel sheet with the same size as the auxiliary electrode with the distance of 5 cm. Electrodeposition was carried out at 60 °C for 1 h with a cathodic current of 50 mA. Finally, the nickel foam substrate was heat treated in a quartz tube furnace at 350 °C for 2 h in flowing argon.

The structure and morphology of the products were characterized by means of X-ray diffraction (XRD, Rigaku D/max–3B),

* Corresponding author. Tel.: +86 571 87952573; fax: +86 571 87952856.
E-mail address: tujp@zju.edu.cn (J.P. Tu).

0378-7753/$ – see front matter © 2008 Elsevier B.V. All rights reserved.
doi:10.1016/j.jpowsour.2008.11.111

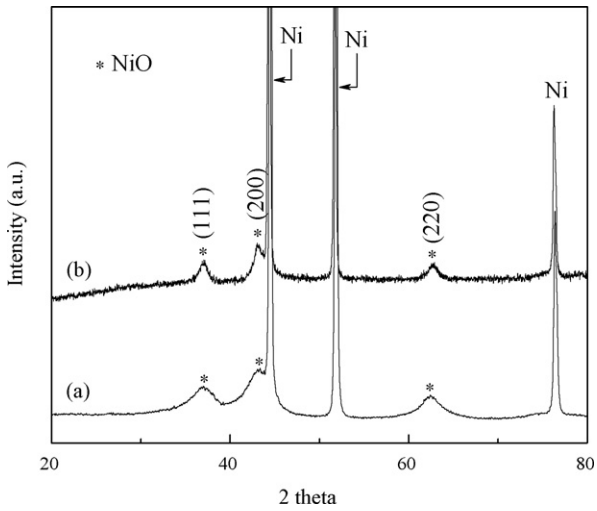

Fig. 1. XRD patterns of the NiO films prepared by (a) chemical bath deposition and (b) electrodeposition.

scanning electron microscopy (SEM, FEI Sirion), and transmission electron microscopy (TEM, JEOL JEM200CX).

Test cells were assembled in an argon-filled glove box using the as-prepared NiO films as working electrode, Li foil as counter electrode, polypropylene film as separator, and an electrolyte of 1 M $LiPF_6$ in a 50:50 (w/w) mixture of ethylene carbonate and diethyl carbonate. The cells were galvanostatically discharged and charged repeatedly at different current densities of 0.5 A g^{-1} and 1.5 A g^{-1} over a voltage of 0.1–3.0 V vs. Li^+/Li. Cyclic voltammetry (CV) tests were carried out using a CHI660C electrochemical workstation at a scanning rate of 0.5 mV s^{-1} between 0 and 3 V.

3. Results and discussion

For the porous NiO film, the reactions in the chemical bath deposition were studied before [13,14]. The first process was that the homogeneous nucleation and precipitation of nickel hydroxide, which can be written as follows:

$$Ni^{2+} + 2OH^- \rightarrow Ni(OH)_2$$

Then the $Ni(OH)_2$ reacted with persulfate on the substrate, and it was oxidized to the higher oxidation states, which can be written as follows:

$$2Ni(OH)_2 + S_2O_8{}^{2-} \rightarrow 2NiOOH + 2SO_4{}^{2-} + 2H^+$$

For the dense NiO film, the electrochemical reactions on the cathode were also studied in earlier works [19–21]. The Ni^{2+} in the solution reacted with OH^-, which was produced by the reduction of $NO_3{}^-$ close to the cathode, forming $Ni(OH)_2$, according to the following reactions:

$$NO_3{}^- + H_2O + 2e^- \rightarrow NO_2{}^- + 2OH^-$$

$$Ni^{2+} + 2OH^- \rightarrow Ni(OH)_2$$

It is reported that during this electrodeposition, the hydroxide films will form at a low specific current density [20,21]. In this case, the cathodic current is only 50 mA, as the specific surface area of the nickel foam is very high, the specific current density is reduced to a low value. So, the nucleation and deposition of $Ni(OH)_2$ is very slow, and results in the formation of the dense film.

XRD patterns of films from the chemical bath deposition and the electrodeposition are given in Fig. 1. Excluding the three strong peaks from the nickel foam substrate, the peaks at 37.3°, 43.3°, and

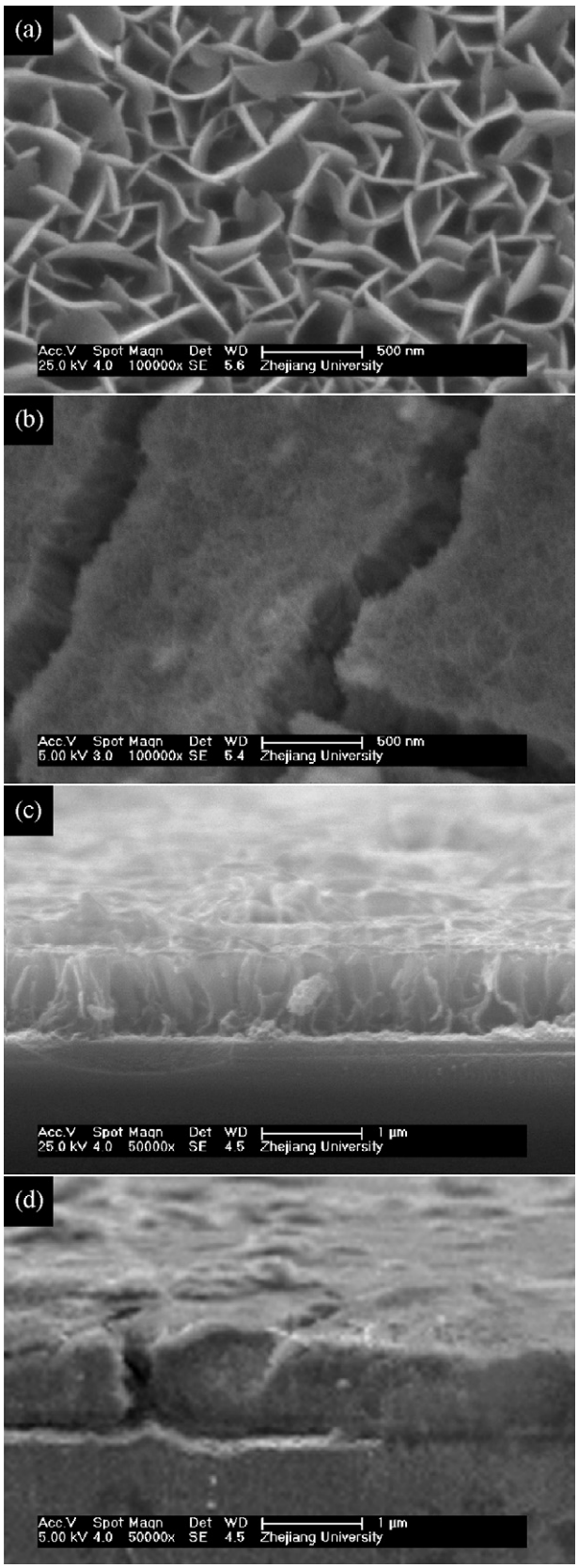

Fig. 2. SEM images of the NiO films prepared by (a) chemical bath deposition and (b) electrodeposition. The cross-sectional SEM images of the NiO films prepared by (c) chemical bath deposition and (d) electrodeposition.

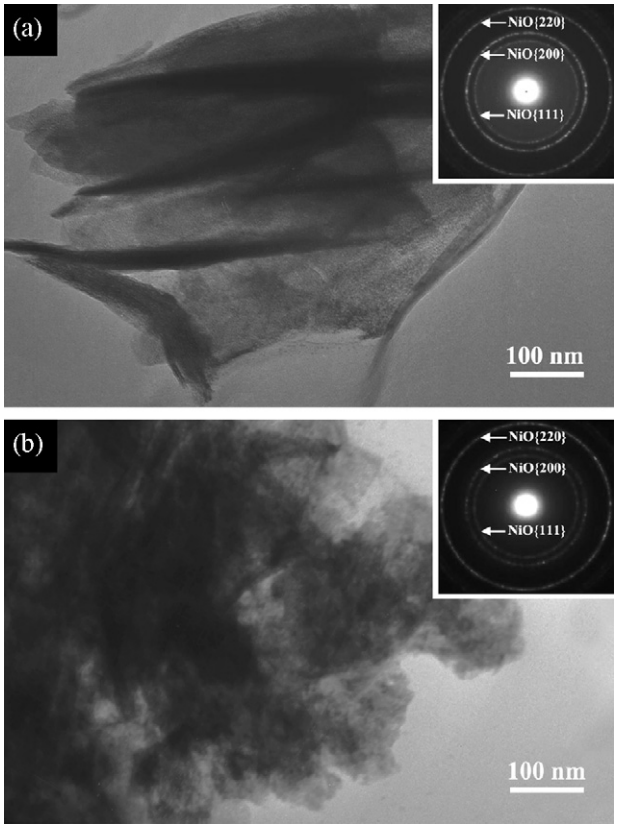

Fig. 3. TEM images of the NiO particles separated from the films prepared by (a) chemical bath deposition and (b) electrodeposition (inserts: SAED patterns).

62.9° in both patterns can be assigned to (1 1 1), (2 0 0), and (2 2 0) reflections of cubic NiO (JCPDS card no. 47-1049), respectively, and no other peaks of impurities can be seen, indicating that the NiOOH and the $Ni(OH)_2$ precursor were completely decomposed to NiO after the heat treatment.

The SEM morphologies of the both films are shown in Fig. 2. The film prepared by chemical bath deposition (Fig. 2a) has a porous morphology, and is constructed by many interconnected nanoflakes with a thickness of about 20 nm. The NiO flakes arrange vertically to the substrate, forming a net-like structure and leaving pores with a size of about 200 nm. However, the film prepared by electrodeposition is dense with no pores in it. As the film is very dense, during the heat treatment, the decomposition of the as-deposited $Ni(OH)_2$ film results in a severe shrinkage, leaving many cracks in the film, as shown in Fig. 2b. The highly porous morphology is beneficial to the electrochemical performance as the porous film has a high specific surface area, which will be discussed later. According to the cross-sectional SEM images, it is clear that both the film prepared by chemical bath deposition (Fig. 2c) and the film prepared by electrodeposition (Fig. 2d) have a thickness of about 1 μm. Fig. 3 gives the TEM images of the particles which were separated from the films by ultrasonic. Fig. 3a shows the image of a NiO nanoflake, and it can be seen that it is very smooth. However, as shown in Fig. 3b, the particles from the dense film are corrugated without any characteristic morphology.

Fig. 4 shows the first discharge–charge curves for the two film electrodes. Both of the films exhibit the first discharge capacity of about 1000 mAh g^{-1}, much higher than the theoretical value (718 mAh g^{-1}), which is due to the formation of solid electrolyte interphase (SEI) in the first discharge, and this happens in all transition-metal oxides including NiO, FeO, CoO and CuO. This SEI layer is a gel-like film which contains ethylene oxide based oligomers, LiF, Li_2CO_3 and lithium alkyl carbonate ($ROCO_2Li$) [22]. The first charge capacity for chemical-bath-deposited film electrode is 700 mAh g^{-1}, leading to the initial coulombic efficiency of 70%. However, for the electrodeposited film, its first charge capacity is only 530 mAh g^{-1}, leading to a much lower initial coulombic efficiency of only 53%. This is because the porous film has a larger contact area between the film and the electrolyte, and a much shorter diffusion length of lithium ions, resulting in a more complete discharge–charge reaction. So the first charge reaction $Ni + Li_2O \rightarrow NiO + 2Li$ can proceed to a higher extent and thus results in higher initial coulombic efficiency. It is obvious that the film prepared by chemical bath deposition shows a higher discharge plateau and a lower charge plateau, indicating smaller potential hysteresis and lower internal resistance of the cell.

Fig. 5 shows the CV curves of the two film electrodes at a scan rate of 0.5 mV s^{-1}. For the chemical-bath-deposited NiO film electrode, a main reduction peak locates around 0.57 V, and a low-density peak near 1.23 V, correspond to the reduction of NiO to metallic Ni nanoparticles and the formation of a partially reversible SEI layer [3]. Three oxidation peaks are well resolved, including a low-density peak around 0.75 V and a broad peak around 1.82 V, corresponding to the partial decomposition of the polymeric coating on the NiO surface, and a broad peak around 2.54 V, corresponding to the decomposition of Li_2O [3,4]. For the electrodeposited NiO film elec-

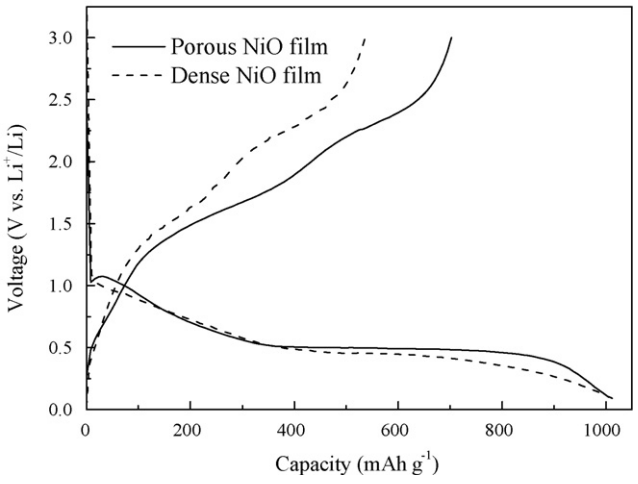

Fig. 4. The comparison of the first discharge–charge curves of the two film electrodes.

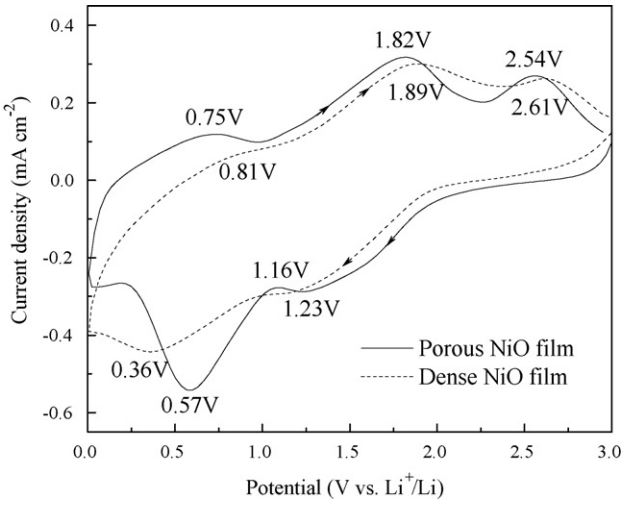

Fig. 5. The comparison of the CV curves of the two film electrodes at the 3rd cycle.

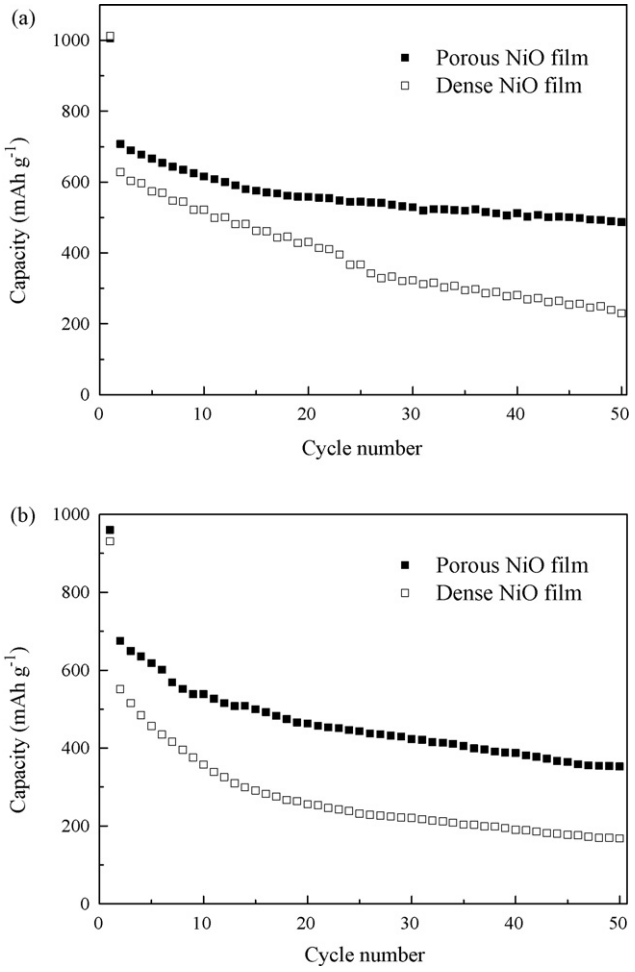

Fig. 6. The cycling performances of the two film electrodes cycled at (a) 0.5 A g^{-1} and (b) 1.5 A g^{-1}.

trode, the two reduction peaks shift to 0.36 V and 1.16 V, and the three oxidation peaks shift to 0.81 V, 1.89 V and 2.61 V, respectively. Obviously, weaker polarization and better reversibility is obtained for the film prepared by chemical bath deposition.

Fig. 6 shows the cycling performance of the two film electrodes. It can be seen that the film prepared by chemical bath deposition has higher reversible capacities and much better capacity retention both in the current densities of 0.5 A g^{-1} and 1.5 A g^{-1}. The specific capacity of the NiO film prepared by chemical bath deposition after 50 cycles is 490 mAh g^{-1} at the current density of 0.5 A g^{-1}, and 350 mAh g^{-1} at 1.5 A g^{-1}. For the electrodeposited film electrode, this capacity is only 230 mAh g^{-1} at 0.5 A g^{-1}, and 170 mAh g^{-1} at 1.5 A g^{-1}. The good capacity retention and rate properties of NiO film prepared by chemical bath deposition are caused by its highly porous structure. The large pores between the nanoflakes result in easy access by the electrolyte, so each nanoflake can be fully immersed in the electrolyte [12]. As the nanoflakes are 20 nm in thickness, the diffusion length of the Li^+ ions is reduced to 10 nm. However, for the dense NiO film, only the surface of the film can be contacted with the electrolyte, and result in a much longer diffusion length of about 1 μm. In addition, the porous film has a high specific surface area, and this will reduce the specific current density in NiO. So it is possible for the porous film to have high specific capacity and good cycling performance at high current density because all the NiO nanoflakes including the surface and the inner parts can react with Li^+ very fast even at high current density. Finally, the porous structure has another advantage, which can result in better performance. As it is knows, the reaction between NiO and Li^+ causes a volume change, but for the porous film, the porous structure can relax the tension caused by this volume change, which is also result in better cycling performance.

4. Conclusions

The porous NiO film and the dense NiO film were prepared by chemical bath deposition and electrodeposition method, respectively. The porous morphology is benefit for the electrochemical performance of the film. The porous NiO film exhibited higher initial coulombic efficiency, weaker polarization, and better cycling performance than the dense film. This is attributed to its porous structure, as the porous film has a high specific surface area, leading to a larger contact area between the film and the electrolyte and a shorter diffusion length of lithium ions, and can also relax the volume change caused by the reaction between NiO and Li^+.

References

[1] P. Poizot, S. Laruelle, S. Grugeon, L. Dupont, J.-M. Tarascon, Nature 407 (2000) 496.
[2] J.-M. Tarascon, M. Armand, Nature 414 (2001) 359.
[3] S. Grugeon, S. Laruelle, R. Herrera-Urbina, L. Dupont, P. Poizot, J.-M. Tarascon, J. Electrochem. Soc. 148 (2001) A285.
[4] A. Débart, L. Dupont, P. Poizot, J.-B. Leriche, J.-M. Tarascon, J. Electrochem. Soc. 148 (2001) A1266.
[5] D. Larcher, G. Sudant, J.-B. Leriche, Y. Chabre, J.-M. Tarascon, J. Electrochem. Soc. 149 (2002) A234.
[6] P. Poizot, S. Laruelle, S. Grugeon, J.-M. Tarascon, J. Electrochem. Soc. 149 (2002) A1212.
[7] Y. Yu, C.-H. Chen, J.-L. Shui, S. Xie, Angew. Chem. Int. Ed. 44 (2005) 7085.
[8] Y. Yu, C.-H. Chen, Y. Shi, Adv. Mater. 19 (2007) 993.
[9] Y. Wang, Q.-Z. Qin, J. Electrochem. Soc. 149 (2002) A873.
[10] Y. Wang, Y.-F. Zhang, H.-R. Liu, S.-J. Yu, Q.-Z. Qin, Electrochim. Acta 48 (2003) 4253.
[11] E. Hosono, S. Fujihara, I. Honma, H. Zhou, Electrochem. Commun. 8 (2006) 284.
[12] E. Hosono, S. Fujihara, I. Honma, M. Ichihara, H. Zhou, J. Electrochem. Soc. 153 (2006) A1273.
[13] P. Pramanik, S. Bhattacharya, J. Electrochem. Soc. 137 (1990) 3869.
[14] S.-Y. Han, D.-H. Lee, Y.-J. Chang, S.-O. Ryu, T.-J. Lee, C.-H. Chang, J. Electrochem. Soc 153 (2006) C382.
[15] X.H. Xia, J.P. Tu, J. Zhang, X.L. Wang, W.K. Zhang, H. Huang, Electrochim. Acta 53 (2008) 5721.
[16] X.H. Huang, J.P. Tu, Z.Y. Zeng, J.Y. Xiang, X.B. Zhao, J. Electrochem. Soc. 155 (2008) A438.
[17] X.H. Huang, J.P. Tu, X.H. Xia, X.L. Wang, J.Y. Xiang, Electrochem. Commun. 10 (2008) 1288.
[18] J. Morales, L. Sánchez, S. Bijani, L. Martínez, M. Gabás, J.R. Ramos-Barrado, Electrochem. Solid-State Lett. 8 (2005) A159.
[19] G.H.A. Therese, P.V. Kamath, Chem. Mater. 12 (2000) 1195.
[20] G. Duan, W. Cai, Y. Luo, F. Sun, Adv. Funct. Mater. 17 (2007) 644.
[21] S.-L. Chou, J.-Z. Wang, H.-K. Liu, S.-X. Dou, J. Power Sources 182 (2008) 359.
[22] G. Gachot, S. Grugeon, M. Armand, S. Pilard, P. Guenot, J.-M. Tarascon, S. Laruelle, J. Power Sources 178 (2008) 409.